17th World Conference on Earthquake Engineering, 17WCEE
Sendai, Japan - September 13th to 18th 2020

EFFICIENT SHEAR-FLEXURE INTERACTION MODEL FOR REINFORCED CONCRETE WALLS

L. Massone[(1)], C. López[(2)], K. Kolozvari[(3)]

[(1)] *Associate Professor, University of Chile, lmassone@uchile.cl*
[(2)] *MSc. Student, University of Chile, carlos.lopez.o@ug.uchile.cl*
[(3)] *Assistant Professor, California State University Fullerton, kkolozvari@fullerton.edu*

Abstract

Reinforced concrete (RC) structural walls are commonly used to resist lateral loads imposed by wind and earthquake ground motions due to their high strength and stiffness. Performance-based methodologies for design require a reliable prediction of nonlinear response of structural elements, thus analytical models that can accurately capture the hysteretic behavior of individual structural members under generalized load conditions are a need. Most of macroscopic models available today can accurately predict flexural behavior for slender walls (flexural models) and are generally computationally efficient and relatively easy to implement. However, these flexural models cannot predict the experimentally observed interaction between flexural and shear behavior in RC walls that can significantly impair the accuracy of the predicted wall behavior in some cases. Nowadays, there are three macroscopic model capable of capturing flexural and shear behavior in walls that are implemented in OpenSees platform: 1) dispBeamColumnInt, 2) truss2, and 3) SFI-MVLEM. However, computational cost makes these models less desirable than simple flexural models, although flexural models do not capture shear behavior. This study deals with development and validation of a modeling approach for RC wall that can accurately capture nonlinear shear and flexural behaviors, even for squat walls, with improved computational efficiency relative to other macroscopic models. This new approach is based on the SFI-MVLEM formulation, which is characterized by six external degrees of freedom (DOFs) that represent horizontal, vertical and rotation at the top and bottom element nodes (for planar structures), to complete the strain field of a constitutive RC panel behavior, an internal DOF in the horizontal direction is added in each one of the panel, imposing a resultant horizontal stress equal to zero (associated to no forces on the sides of the walls). Thus, each element consists of 3 DOFs per node, plus the *m* number of RC panel elements per model element (usually over 8 for a good discretization). The new approach with the calibrated expression for the horizontal expansion allows to remove the *m* internal DOFs within each element, resulting in the same number of DOFs as flexural models, reducing the size of the element stiffness matrix in comparison to original SFI-MVLEM. In this case, the horizontal strain is determined for each step and each panel based on the shear and normal vertical strains for a database of 2D-FEM models with 262 cases. The shear strength predicted by the model is contrasted with a large database of wall specimens collected from the literature (252), indicating an accurate prediction of the model for a wide range of shear span-to-depth ratio. Also, the model is validated against cyclic response of a slender and a squat wall, obtaining a consistent prediction of the global response, as well as, flexural and shear behavior for both cases.

Keywords: RC Walls; Nonlinear Analysis; OpenSees; Shear; Flexure.

1. Introduction

Reinforced concrete (RC) walls are commonly used in structural configurations that require limit lateral deformations and to resist the actions due to lateral loads as imposed by earthquake ground motions and wind loads. Reliable prediction of nonlinear behavior of structural elements is required for performance base design, thus robust modeling and analysis tools that can accurately capture the hysteretic behavior of structural elements are a need. An effective analytical model should be relatively simple to implement and reasonably accurate predicting the nonlinear hysteretic response of RC wall systems at both local and global levels, as well as capturing the interaction of the walls with other structural members [1].

Test results of specimen RW2 (Fig. 1) reveals that inelastic behavior of flexural and shear response occurs near simultaneously at a lateral load close to the wall nominal moment (131 kN) despite wall nominal shear capacity (Vn = 276 kN) of approximately twice the applied story shear (133 kN) [2]. The observed results clearly demonstrate an interaction between shear and flexural response, indicating that inelastic flexural deformations led to near-simultaneous inelastic shear deformations, commonly referred as shear-flexure interaction (SFI).

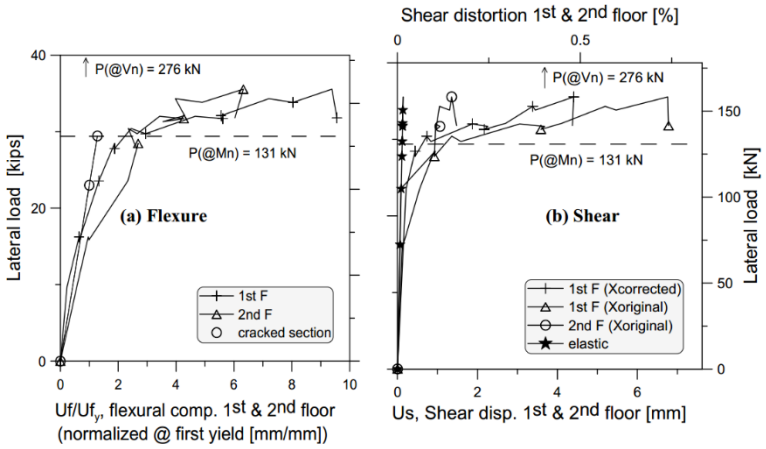

Fig. 1 – First and second story deformations for RW2 specimen test [2].

Although RC wall specimens test have shown that shear and axial/flexural deformation interaction exist even for relative slender walls dominated by flexural yielding, separating the shear and flexural behavior is a common practice. Analytical modeling of inelastic response of structural wall systems can be accomplished by using microscopic (finite element) or macroscopic (behavioral) models. For finite element model (FEM), shear-flexure interaction can be captured, however, due to high computational cost and complexity in their implementation, this type of model is less used compared to behavioral models.

Most of macroscopic models available nowadays do not account for shear-flexure interaction (flexural models) as the MVLEM [1,3], which is adequate for relative slender walls but becomes relevant for low aspect ratio walls or walls segments due to a high contribution of nonlinear shear response. Nowadays exist three models in OpenSees platform that include shear-flexure interaction: 1) dispBeamColumnInt [2,4], 2) truss2 [5,6], and 3) SFI-MVLEM [7,8], however, computational cost makes this type of models less desirable than simple flexural models, although flexural models do not capture accurately nonlinear hysteretic behavior, especially for squat walls.

2. Analytical model description and background

This new analytical model called Efficient-Shear-Flexure-Interaction (ESFI) is based on the Shear-Flexure-Interaction-Multiple-Vertical-Line-Element-Model (SFI-MVLEM), which formulation incorporates the RC panel behavior to include the shear-flexure interaction as proposed by the dispBeamColumnInt model, which in turn is based on Multiple-Vertical-Line-Element-Model (MVLEM) formulation.

The MVLEM is described by six external DOFs that represent horizontal, vertical and rotation at the top and bottom element nodes $\{\delta_N\}$, which makes possible to compute the vertical strain of each one of the *m* uniaxial elements over the wall length considering that plain section remains plain, and the shear strain for the shear spring placed at height *ch* (Fig. 2a). The curvature is assumed to be uniform and concentrated at the center of rotation *ch* and a value of $c = 0.4$ was recommended based on comparison with experimental results [1]. Because of shear and axial/flexural behaviors are described independently, experimentally observed shear-flexure interaction cannot be captured and nonlinear response is accurately predicted only for slender walls. The total number of degrees of freedom in a complete wall model is $N=3(n+1)$, where *n* is the number of vertical MVLEM elements in the wall. The global stiffness matrix $[K]$ is a square matrix of dimension NxN and the global force vector $\{F_{int}\}$ is a vector of dimension Nx1, the nonlinear problem to solve consist in reaching the force equilibrium in each one of the *N* degrees of freedom.

The dispBeamColumnInt model includes the experimentally observed shear-flexure interaction replacing the *m* uniaxial elements of the MVLEM by two-dimensional RC panel elements (also called strips) subjected to membrane actions with a rotating-angle modeling approach. Element strains are determined with the six prescribed DOFs (similar DOFs as MVLEM), obtaining the axial strain (ε_y) and shear distortion (γ_{xy}) for the entire section, to complete the strain field, the horizontal normal strain (ε_x) is estimated for each strip (Fig. 2b). A numerical procedure is implemented to iterate over the unknow quantity ε_x to achieve resultant horizontal normal stress (σ_x) equilibrium within each strip. This model enforces zero resultant horizontal normal stress, which assumption is accurate for mid-slender to slender wall [4].

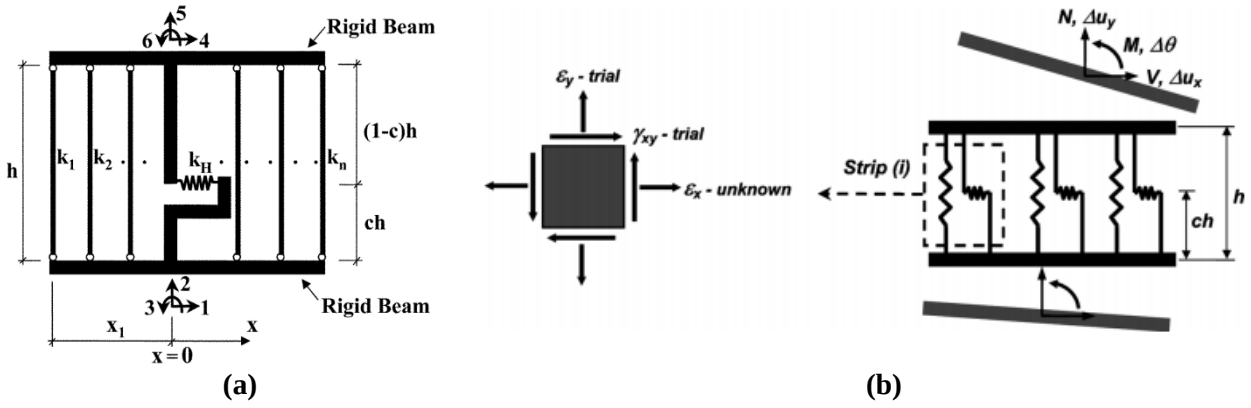

Fig. 2 – (a) MVLEM Element [1]; (b) RC panel incorporation at strip level [4].

The SFI-MVLEM adopts the formulation proposed by the dispBeamColumnInt model, although some changes are adopted to include the cyclic response and to improve computation efficiency of the model. To incorporate the cyclic response, the RC panel rotating-angle modeling approach was changed to the Fixed-Strut-Angle-Model (FSAM) [9] and, to improve computation efficiency, a horizontal DOF is added in each strip to compute the unknow quantity ε_x, enforcing zero resultant horizontal normal stress (Fig. 3a). Thus, the model is defined by the same six external DOFs $\{\delta_N\}$ as the MVLEM plus *m* number of internal DOFs $\{\delta_x\}$. The total number of degrees of freedom in the complete wall model is $N=3\cdot(n+1)+m\cdot n$, where *n* is the number of vertical SFI-

MVLEM elements in a wall. The size of the problem to solve is increased by $m \cdot n$, which together with the RC panel constitutive behavior, results in a more complex and computationally costly element than the MVLEM.

The developed two-dimensional macroscopic model ESFI (Fig. 3b) uses m RC Panel with a cyclic response described by the FSAM to incorporate the shear flexure interaction. To complete the strain field of a constitutive RC panel behavior, a calibrated expression of the normal horizontal strain in terms of normal vertical and shear strain is adopted, in order to obtain accurate results for squat and slender RC walls. Thus, the model is defined only by the same six external DOFs $\{\delta_N\}$ as the MVLEM. The total number of degrees of freedom in the complete wall model is $N=3\cdot(n+1)$, where n is the number of vertical ESFI elements in a wall. The size of the problem is reduced by $m \cdot n$ in contrast to the SFI-MVLEM, resulting in the same number of DOFs as the MVLEM, thus, computational cost is reduced.

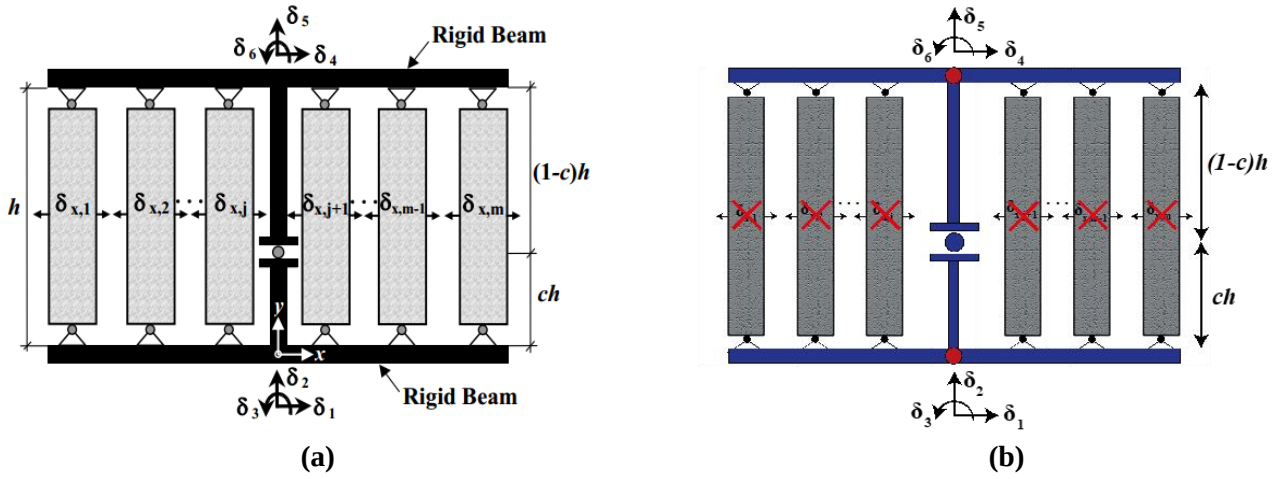

Fig. 3 – Degrees of freedom of: (a) SFI-MVLEM [7]; (b) ESFI element.

3. Calibration of the horizontal normal strain

The calibration of the horizontal normal strain to complete the strain field of the RC panel behavior is obtained using a conventional two-dimensional finite element model (2D-FEM) formulation as described by Massone [10]. The 2D-FEM RC wall models are discretized in a series of 4-nodes rectangular elements that are connected to each other. The 4-nodes elements use a linear interpolation between the nodal displacements and consider reduced integration (one Gauss point at element centroid). The model material is described by a RC panel behavior and the horizontal normal strain is part of the equilibrium equation, then, no assumptions are required. The 2D-FEM considers two traditional boundary conditions, single curvature (or cantilever) and double curvature (or zero-end rotation condition), and the response is analyzed varying different parameters such as: aspect ratio (h_w/l_w), vertical web distributed reinforcement ratio (ρ_{wv}), horizontal web distributed reinforcement ratio (ρ_{wh}), longitudinal boundary reinforcement ratio (ρ_b), axial load (N), compressive strength of concrete (f'_c) and yield strength of steel (f_y). The range of values selected for each parameter was: h_w/l_w = 0.33 to 1.4; ρ_{wh} = 0 to 1%; ρ_{wv} = 0 to 1%; ρ_b = 1 to 6%; N = 0 to $0.3A_g f'_c$ (where A_g corresponds to wall cross-sectional area); f'_c = 30 to 50 MPa and f_y = 280 to 420 MPa. For each boundary condition a total number of 131 cases was analyzed, resulting in a total number of 262 2D-FEM RC walls analysis. Detailed information and validation of the 2D-FEM RC wall models can be found in the publication by Massone [10].

In this approach for the calibration of the horizontal normal strain, a linear regression is used considering only local responses such us: vertical normal strain and shear strain, using the data provided by the 2D-FEM RC wall analysis without distinction between different boundary conditions and wall parameters (Fig. 4a). The

fitted curve is selected for the best R-squared (R^2) value, obtaining the expression shown in Eq. (1), which R^2 value is 0.79.

$$\varepsilon_x = -0.166 \cdot |\varepsilon_y| + 0.444 \cdot |\gamma_{xy}| \quad (1)$$

For test number 20 of the 2D-FEM RC wall test database, the mean normal horizontal strain over the height obtained by the FEM model and the calibrated expression (CAL) at different drift levels (δ) are presented in Fig. 4b, indicating a good estimation of ε_x, although better estimations are obtained as drift level are increased, this behavior is observed in most of 262 2D-FEM RC walls analysis.

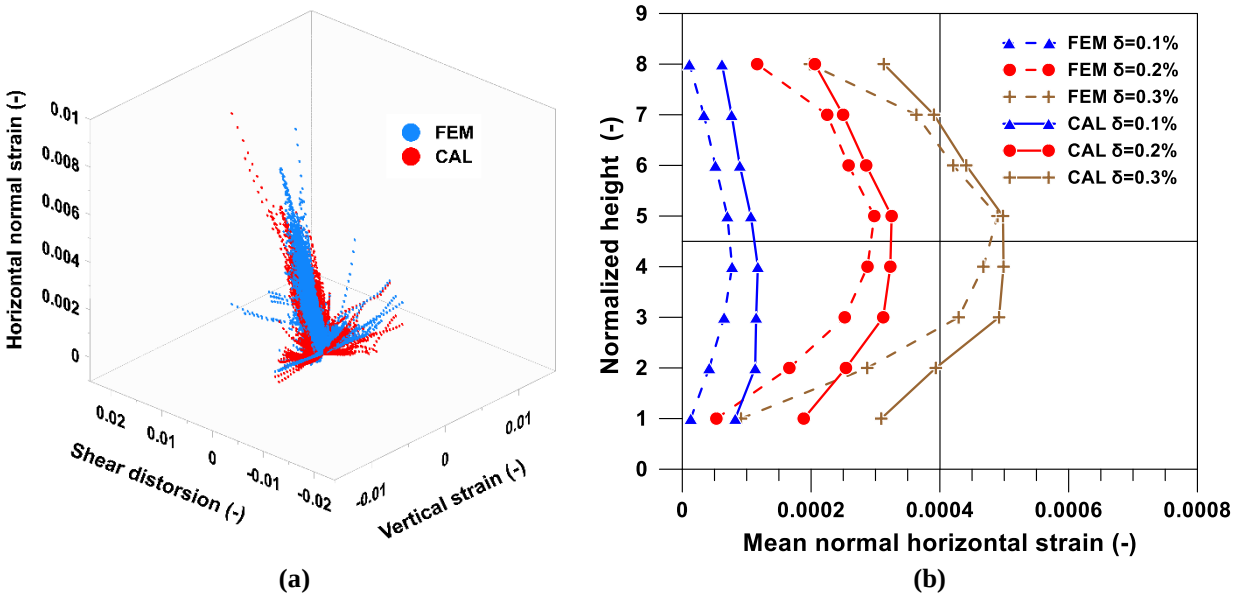

Fig. 4 – (a) Data points for calibration of the horizontal normal strain; (b) Mean normal horizontal strain profile for test N°20 of the 2D-FEM RC wall test database at different drift levels.

4. Shear strength test database comparison

The calibration shown in Eq. (1) is implemented in the shear-flexure interaction model ESFI, and the shear strength prediction obtained by the model is compared to a large database of 252 wall test data reported in the literature. The database includes the work summarized by Hirosawa [11] and Mohammandi-Doodstdar and Saatciouglu [12], and the publication by Massone et al. [13], Hidalgo et al. [14], Yamada et al. [15], Antebi et al. [16], Barda et al. [17], Benjamin and Williams [18], Cardenas et all [19], and Galletly [20].

The RC wall models were discretized in eight vertical elements and eight horizontal fibers resulting in a total of 64 panels elements and 27 DOFs. The selected constitutive material for concrete was Chang and Mander (Fig. 4a), whereas constitutive material for steel was Manegotto and Pinto Model Extended by Filippou et al. (Fig. 4b) as it is used by the SFI-MVLEM [8]. The computational model tests with cantilever boundary condition were free to rotate at wall top end, whereas double curvature boundary condition tests were restrained to rotate at wall top end. The analysis was performance using a displacement-controlled analysis to obtain the maximum lateral force attained, that is, the shear strength of the wall.

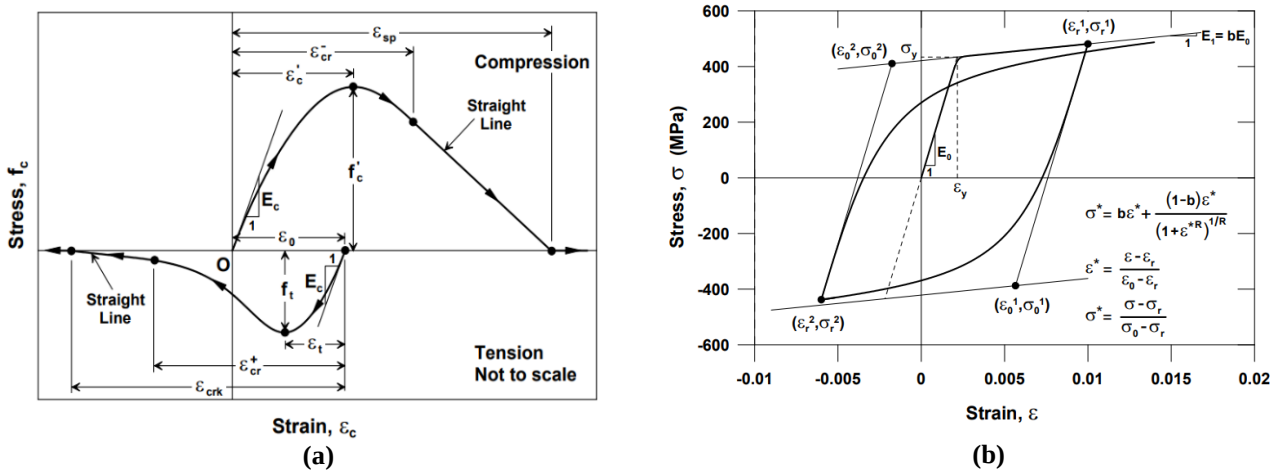

Fig. 5 – Hysteretic constitutive model for: (a) concrete by Chang and Mander; (b) steel by Manegotto and Pinto, extended by Filippou et al. [8]

The ratio of the predicted over the experimental shear strength, or strength ratio, was determined for all cases (V_{model}/V_{test}). The average strength ratio obtained using the ESFI model was 0.96, with a standard deviation of 0.25 and a coefficient of variation of 0.26, indicating a good correlation of the computational model with test result, and a relatively small dispersion. The maximum strength ratio was 1.82, whereas the minimum value was 0.49, however, most amount of strength ratios range between 0.6 to 1.4 (90%).

Fig. 5 shows the model prediction sensitivity to the shear span-to-depth-ratio ($M/(Vl_w)$) of the wall, the horizontal dotted line indicates a perfect correlation between the model and the test ($V_{model}/V_{test} = 1$). The ESFI trend indicates a slightly dependence of the model with this parameter (with a variation of approximately 10% over the hole range). A good correlation is obtained for a shear span-to-depth-ratio near zero and a slightly conservative prediction of the model is obtained as the parameter increases.

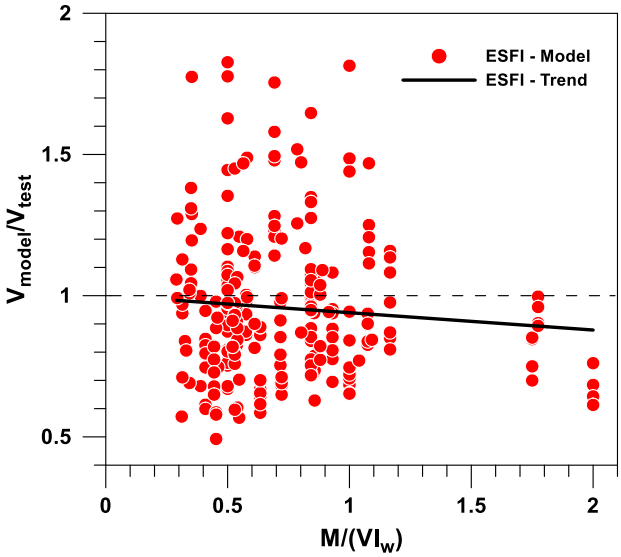

Fig. 5 – Shear strength ratio (V_{model}/V_{test}) vs. shear span-to-depth ratio.

5. Cyclic response comparison

To demonstrate the robustness of the ESFI model to cyclic response, two RC wall test that represents a wide range of shear span-to-depth ratio are used, RW2 ($M/(Vl_w)$ = 3.0) by Thomsen and Wallace [21] and WP-T5-N0-S1 ($M/(Vl_w)$ = 0.44) by Massone [2], which properties are presented in Table 1.

RW2 wall (Fig. 6a), was a specimen with rectangular cross section and single curvature boundary condition. The wall was 3.66 m tall, 102 mm thick and 1.22 m length, subjected to a constant axial vertical load of $0.07A_g f'_c$ and a reversed cyclic lateral load at top of the wall. Boundary elements were provided at the edge of the wall over the bottom 1.22 m. Transverse and longitudinal web reinforcement ratio of 0.325% were provided, while boundary reinforcement ratio was 2.93%.

WP-T5-N0-S1 wall (Fig. 6b), was a specimen with rectangular cross section and double curvature boundary condition. The wall was 1.22 m tall, 152 mm thick and 1.37 m length, subjected to a reversed cyclic lateral load at the mid-height of the wall in addition to a system to restrain rotations at top of the wall. Transverse and longitudinal web reinforcement ratio of 0.278 and 0.227% were provided respectively, while boundary reinforcement ratio was 1.33%.

Table 1 – RC wall specimen's properties

Specimen ID	Geometric properties			Transverse web reinforcement		Longitudinal web reinforcement		Boundary reinforcement		Axial Load	Concrete properties	
	t_w, cm	l_w, cm	h_w, cm	ρ_{wh}, %	f_y, MPa	ρ_{wv}, %	f_y, MPa	ρ_b, %	f_y, MPa	$N/f'_c A_g$, %	f'_c, MPa Bound.	f'_c, MPa Web
RW2	10.2	122	366	0.325	336	0.325	336	2.93	395	7	47.6	42.8
WP-T5-N0-S1	15.2	137	122	0.278	424.0	0.227	424.0	1.33	424.0	0	29.9	29.9

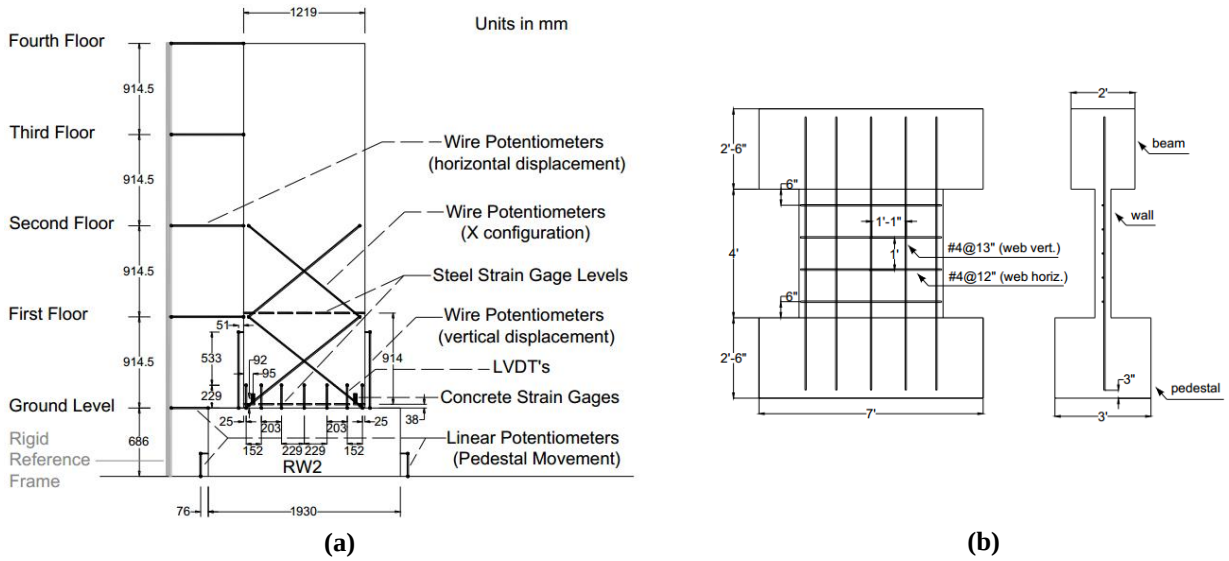

(a) (b)

Fig. 6 – RC wall specimens: (a) RW2 [7]; (b) WP-T5-N0-S1 [2].

5.1 Lateral load vs. top displacement response

Experimentally measured lateral load vs. top displacement responses for specimens RW2 and WP-T5-N0-S1 are contrasted to computational prediction of the ESFI model in Fig. 7. As it can be seen in the figure, global response of the wall using the ESFI model is reasonably accurate for both specimens, although initial stiffness of the wall is slightly over predicted. For RW2 specimen (Fig. 7a), the shear strength predicted by the model shows an error of about 2%, with a slightly capacity degradation at last cycles, which is consistent with test result. In the case of WP-T5-N0-S1 (Fig. 7b), shear strength is overestimated by approximately 5%. The model shows lateral load degradation, which is consistent with test results, although degradation is more gradual in the model prediction. Additionally, global response using the MVLEM is included in the figure, proving that flexural models only capture accurately the response for slender walls, and a shear-flexure interaction model is required to improve computational prediction of hysteretic response, especially for squat walls.

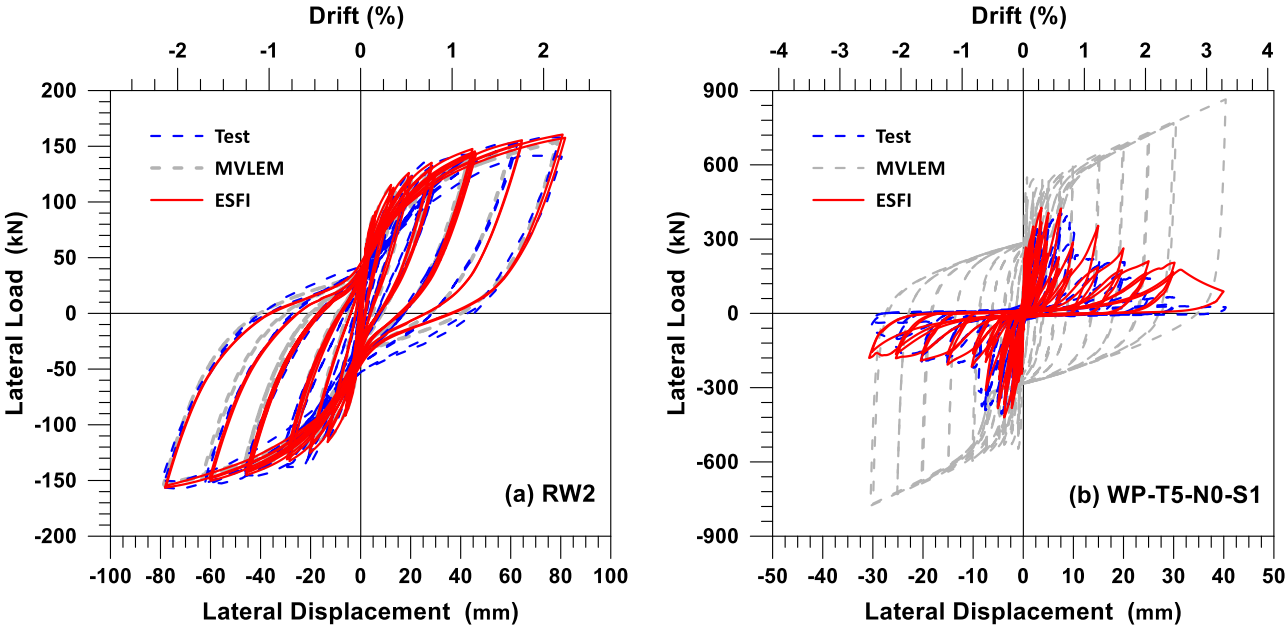

Fig. 7 – Lateral load vs. lateral displacement responses for specimens: (a) RW2; (b) WP-T5-N0-S1

5.2 Flexural and shear deformation components

Model prediction of flexural and shear behaviors are compared with measured response of RC wall specimens (Fig. 8). For RW2 specimen, flexural and shear displacements are measured at first story level (at bottom quarter of the wall), whereas for WP-T5-N0-S1 specimen, flexural and shear components are measured at top of the wall, although a limit number of cycles are compared due to instrumentation problems, as can be seen in Fig. 8c.

In the case of the slender wall, RW2 (Fig. 8a and 8b), flexural displacements at first story are slightly overestimated (about 20%), showing similar ratio between flexural and shear component distribution. Displacements component predicted with the model for the squat wall specimen, WP-T5-N0-S1 (Fig. 8c and 8d), reveal an accurate prediction of flexural and shear behavior, indicating the model ability to predict nonlinear hysteretic behavior including the shear-flexure interaction for squat and slender RC walls.

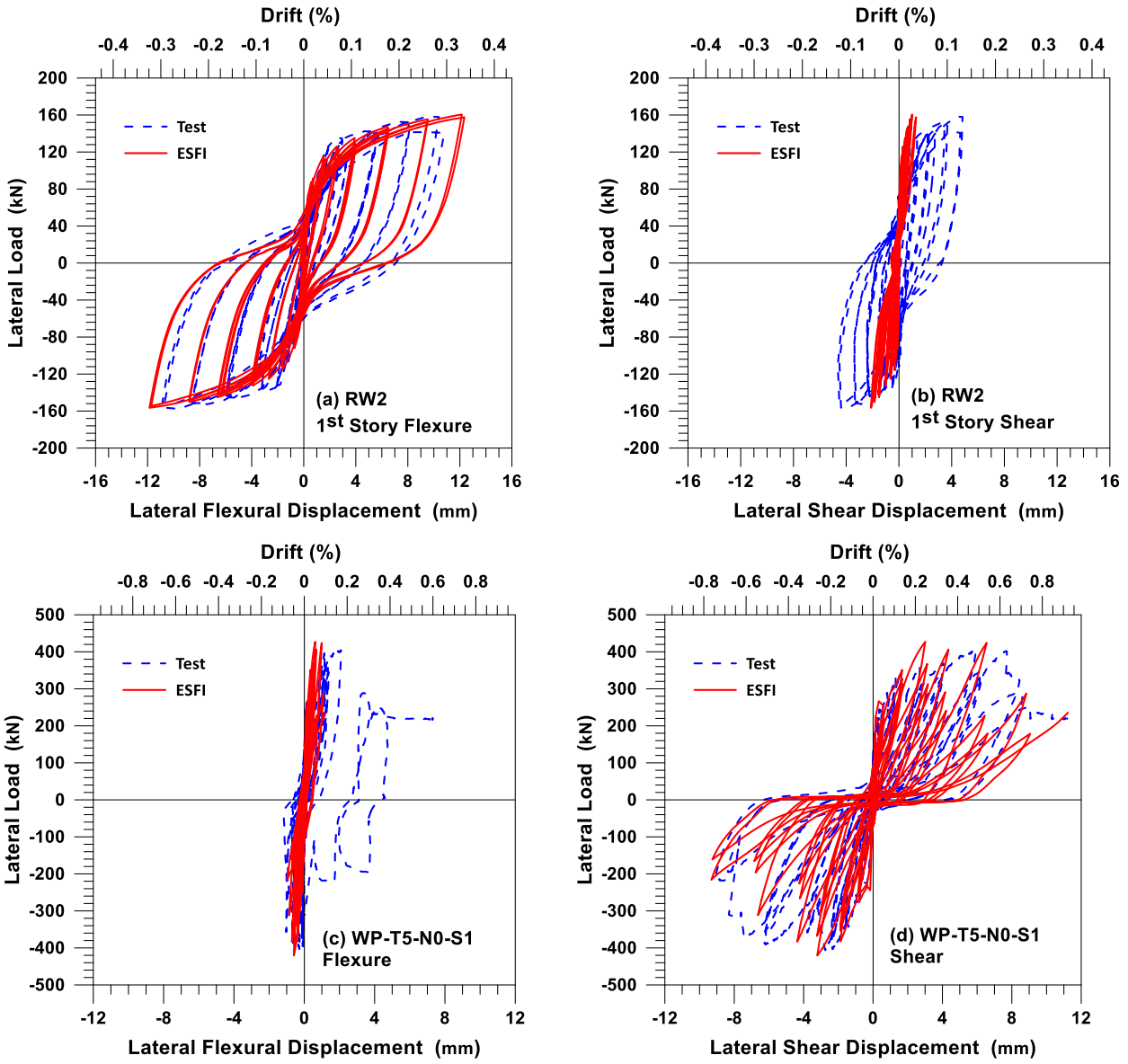

Fig. 8 – Lateral load vs. flexural and shear displacement responses for specimens: (a) RW2 flexural behavior at 1st story; (b) RW2 shear behavior at 1st story; (c) WP-T5-N0-S1 flexural behavior; (d) RW2 shear behavior.

6. Summary and conclusions

A novel macroscopic model called Efficient-Shear-Flexure-Interaction (ESFI), that will be available in OpenSees platform, is proposed to predict nonlinear hysteretic behavior from squat to slender RC walls under reversed cyclic loading conditions. The model includes the experimentally observed shear-flexure interaction by incorporating the RC panel behavior described by the Fixed-Strut-Angle-Model into the MVLEM formulation. To complete the strain field for the RC panel behavior, a calibrated expression for the horizontal normal strain (ε_x) in terms of the axial strain (ε_y) and shear distortion (γ_{xy}) is proposed based on two-dimensional finite element model results, allowing to reduce degrees of freedom compared with actual models that includes the shear-flexure interaction as the SFI-MVLEM. The DOF reduction results in less computation

cost. The shear strength predicted by the model is contrasted with a database of experimental results with a wide range of shear span-to-depth ratio, showing good results over the range with a slightly conservative prediction as the parameter increases. The reversed cyclic response is contrasted for RW2 and WP-T5-N0-S1 specimen tests (shear span-to-depth ratio of 3.0 and 0.44 respectively), obtaining accurate results in the prediction of global, flexural and shear response of the walls, proving the ability of the model to be used in slender and squat RC walls.

7. References

[1] Orakcal, K., & Wallace, J. W. (2006). Flexural modeling of reinforced concrete walls - Experimental verification. *ACI Structural Journal*, *103*(2), 196–206.

[2] Massone LM (2006). RC wall shear–flexure interaction: analytical and experimental responses, PhD Dissertation. University of California, Los Angeles.

[3] Vulcano, A., Bertero, V. V., & Colotti, V. (1988). Analytical modeling of R/C structural walls. In *9th World Conference on Earthquake Engineering* (pp. 41–44).

[4] Massone, L. M., Orakcal, K., & Wallace, J. W. (2006). Shear-flexure interaction for structural walls. *ACI Symposium Publication*, *236*, p. 127–150.

[5] Panagiotou, M., Restrepo, J. I., Schoettler, M., & Kim, G. (2012). Nonlinear cyclic truss model for reinforced concrete walls. *ACI Structural Journal*, *109*(2), 205–214.

[6] Lu, Y., & Panagiotou, M. (2014). Three-dimensional cyclic beam-truss model for nonplanar reinforced concrete walls. *Journal of Structural Engineering (United States)*, *140*(3).

[7] Kolozvari K (2013). Analytical modeling of cyclic shear-flexure interaction in reinforced concrete structural walls, PhD Dissertation. University of California, Los Angeles.

[8] Kolozvari, K., Orakcal, K., & Wallace, J. W. (2015). Modeling of cyclic shear-flexure interaction in reinforced concrete structural walls. I: Theory. *Journal of Structural Engineering (United States)*, *141*(5).

[9] Ulugtekin, D. (2010), Analytical modeling of reinforced concrete panel elements under reversed cyclic loadings, M.S. Thesis. Department of Civil Engineering, Bogazici University.

[10] Massone, L. M. (2010). Strength prediction of squat structural walls via calibration of a shear-flexure interaction model. *Engineering Structures*, *32*(4), 922–932.

[11] Hirosawa, M. (1975). Past experimental results on reinforced concrete shear walls and analysis on them. *Kenchiku Kenkyu Shiryo, No. 6*. Tokyo: Building Research Institute, Ministry of Construction, p. 277 [in Japanese].

[12] Mohammandi-Doostdar, H., & Saatcioglu, M. (2002). Behavior and design of earthquake resistant low-rise shear walls. *Report OCCERC 02-28*. Ottawa Carleton Earthquake Engineering Research Center. Department of Civil Engineering, University of Ottawa, Canada, p. 250.

[13] Massone, L. M., Orakcal, K., & Wallace, J. W. (2009). Modeling of squat structural walls controlled by shear. *ACI Structural Journal*, *106*(5), 646–655.

[14] Hidalgo, P. A., Ledezma, C. A., & Jordan, R. M. (2002). Seismic behavior of squat reinforced concrete shear walls. *Earthquake Spectra*, *18*(2), 287–308.

[15] Yamada, M., Katagihara H., & Katagihara, K. (1974). Reinforced Concrete Shear Walls Without Openings; Test and Analysis. *ACI Symposium Publication*, *42*, p. 539–558.

[16] Antebi, J., Utku, S., & Hansen, R. J. (1960). The response of shear walls to dynamic loads. Department of Civil and Sanitary Engineering, Massachusetts Institute of Technology, Cambridge.

[17] Barda, F., Hanson, J. M., & Corley, W. G. (1977). Shear Strength of Low-Rise Walls with Boundary Elements. *ACI Symposium Publication*, *63*, p. 149–202.

[18] Benjamin, J. R., & Williams, H. A. (1957). The behavior of one-story reinforced concrete shear walls. *Journal of the Structural Division; 83(3)*, p. 1–49.

[19] Cardenas, A. E., Rusell H. G., & Corley W. G. (1980). Strength of low-rise structural walls. *ACI Symposium Publication, 63*, p. 221–242.

[20] Galletly, G. D. (1952). Behavior of reinforced concrete shear walls under static load. Department of Civil and Sanitary Engineering, Massachusetts Institute of Technology, Cambridge.

[21] Thomsen, J. H., & Wallace, J. W. (1995). Displacement-based design of RC structural walls: an experimental investigation of walls with rectangular and T-shaped cross-sections. Department of Civil Engineering, Clarkson University, Postdam, New York, 353 pp.

